ISSN 2616-5880 Vol. 6, Issue 2: 17-24, DOI: 10.25236/AJMC.2025.060202

Effect of Homogenization Annealing Process on Microstructure and Mechanical Properties of 8021 Aluminum Alloy

Zuo Yuan[a,*], Cao Shimin[b], Zeng Yuan[c]

Jiangsu Dingsheng New Energy Materials Co., Ltd., Zhenjiang, 212001, Jiangsu, China
[a]451909269@qq.com, [b]shimin.Cao@dingshenggroup.com, [c]727907713@qq.com
**Corresponding author*

Abstract: *This paper investigates the homogenization annealing of 8021 aluminum alloy after a single deformation at different temperatures. The microstructures of the annealed sheets were characterized using techniques such as EDS, BSE, and SEM. The results show that after homogenization annealing, the tensile strength and yield strength of the material significantly decreased, while the elongation rate markedly improved. Furthermore, as the homogenization temperature increased, the grain size of the final sheets gradually decreased, and the strength also increased with the rise in homogenization temperature. These findings provide important experimental insights for optimizing the heat treatment process of 8021 aluminum alloy.*

Keywords: *8021 aluminum alloy; homogenization annealing; microstructure; grain size; mechanical properties*

1. Introduction

Homogenization annealing is commonly applied to aluminum foil ingots, cast-rolled aluminum foil blanks, or cold-deformed cast-rolled aluminum foil blanks. For 8xxx series alloys, homogenization annealing is typically conducted at 500–600℃, though the temperature may vary depending on alloy composition [1, 2]. Due to the inhomogeneous microstructure of cast-rolled blanks, coarse recrystallized grains are prone to form on the sheet surface, leading to severe surface quality issues [3]. The primary objectives of homogenization annealing are to reduce microsegregation formed during casting, promote the dissolution and reprecipitation of metastable phases to alter their distribution and morphology, and thereby regulate the size and quantity of recrystallized grains in cast-rolled blanks [4, 5].

Researchers have extensively studied the evolution of second phases and grain structures during homogenization annealing of cast-rolled aluminum foils. In cast-rolled blanks, unstable ternary β_p primary phases gradually transform into stable α_c and β_b phases during homogenization annealing, while metastable binary Al_mFe, Al_6Fe, and Al_xFe phases transition into stable Al_3Fe phases [6]. With sufficient heating time, α_c phases ultimately transform into Al_3Fe phases [7].

Kumar et al. [7] investigated the effects of homogenization on the microstructure and texture evolution of twin-roll cast Al-Fe-Si aluminum alloy (AA8011). After homogenization of cold-rolled sheets (50% deformation), Al-Fe-Si ternary phase particles became finer (~2 μm) and more uniform. The near-acicular second phases in the deformed structure transformed into rounded shapes, enhancing deformability. However, centerline segregation (CLS) persisted even after homogenization. Homogenization at 580℃ for 4 h, 8 h, and 12 h strengthened the cube texture and weakened the strong deformation texture, which plays a critical role in material formability. Králík et al. [8] studied the evolution of second-phase particles during homogenization annealing of AA8079 packaging foil. Figure 1-6 shows in-situ heating TEM observations: at 475℃ homogenization, new second-phase particles nucleated within eutectic cells initially free of such particles. Initial particles underwent spheroidization and partial dissolution at 525℃ and 550℃. Dissolution accelerated above 550℃, promoting the growth of large second-phase particles.

In summary, different homogenization temperatures result in distinct second-phase structures and distributions, significantly influencing the quality control of cast-rolled sheets. This study aims to investigate the effects of homogenization annealing processes on the microstructure and mechanical properties of 8021 alloy cast-rolled blanks. Specifically, after identical pretreatment deformation on cast-

ISSN 2616-5880 Vol. 6, Issue 2: 17-24, DOI: 10.25236/AJMC.2025.060202

rolled blanks with the same initial thickness, different homogenization annealing treatments are applied to the deformed substrates to analyze the resulting microstructural and mechanical behavior.

2. Experimental Methods

2.1 Process Route

Figure 1 illustrates the experimental procedure. A thinner 6.0 mm blank was pre-deformed to 4.2 mm, followed by homogenization annealing at 500°C, 540°C, and 580°C for 3 h. The heat-treated sheets were air-cooled, then finally cold-rolled to 1 mm, and annealed at 350°C for 3 hours to comparatively study the influence of homogenization processes on the microstructure. Homogenization annealing experiments were conducted in a TSX 1600 muffle furnace. All observed surfaces in this study were the RD-ND plane.

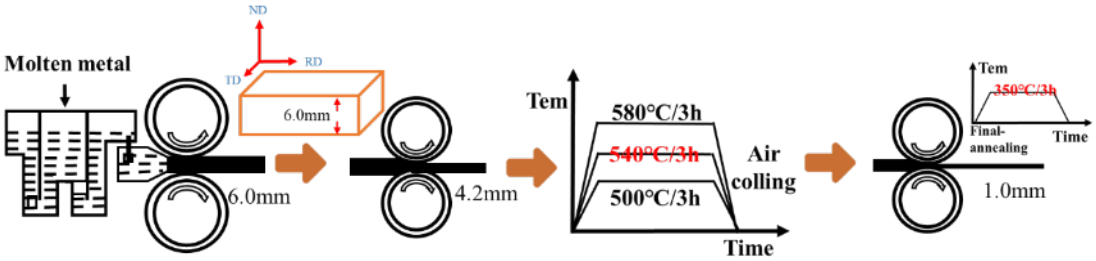

Figure 1 Aluminum alloy rolling process

2.2 Testing Methods

2.2.1 Polarized Optical Microscopy (POM) Observation

Polarized optical microscopy (POM) was used to examine the grain morphology and distribution of the samples. The observed surfaces were primarily longitudinal sections (RD-ND plane), with some samples observed on the rolling plane (RD-TD plane). Prior to observation, the samples underwent an anodic coating process using an electrolytic setup. The coating solution (composition: 38% H_2SO_4 + 43% H_3PO_4 + 19% H_2O) was applied at a voltage of 15–25 V, current density of 0.1–0.5 A/cm², and duration of 1–2 minutes. The coated samples were then observed under a polarized optical microscope (EISS-AXio Observer 3m).

2.2.2 Backscattered Electron (BSE) and Energy-Dispersive Spectroscopy (EDS) Analysis

Backscattered electron (BSE) imaging was employed to characterize the morphology, size, and distribution of second-phase particles within the material. Five BSE images per condition were statistically analyzed using ImageJ. A TESCAN S8000 GMH field-emission scanning electron microscope (SEM) was used for imaging, and an energy-dispersive spectrometer (EDS) was utilized for qualitative analysis of the elemental composition of second phases.

2.2.3 Mechanical Property Testing

Tensile testing of the aluminum sheets was conducted following the YB/T 4334-2013 standard "Metallic Foil Tensile Testing Method at Room Temperature" (equivalent to ASTM E8/E8M). Specimens were cut along the rolling direction (RD), and three measurements were averaged for each condition. The tests were performed using an AG-X plus electronic universal testing machine.

3. Experimental Results and Analysis

3.1 Microstructural Analysis of Cast-Rolled Blanks

The grain distribution of the 6.0 mm cast-rolled blank is shown in Figure 2, observed on the RD-ND plane. Figure 2(a, b) displays the anodized coating images of the edge and core regions of the cast-rolled blank. The macrostructure reveals that the cast-rolled microstructure features surface columnar grains symmetrically distributed along the thickness centerline, transitioning gradually to equiaxed grains in the central region. The orientation of surface columnar grains is approximately 15°–20° relative to the

ISSN 2616-5880 Vol. 6, Issue 2: 17-24, DOI: 10.25236/AJMC.2025.060202

centerline, a characteristic attributed to the rapid solidification during the cast-rolling process.

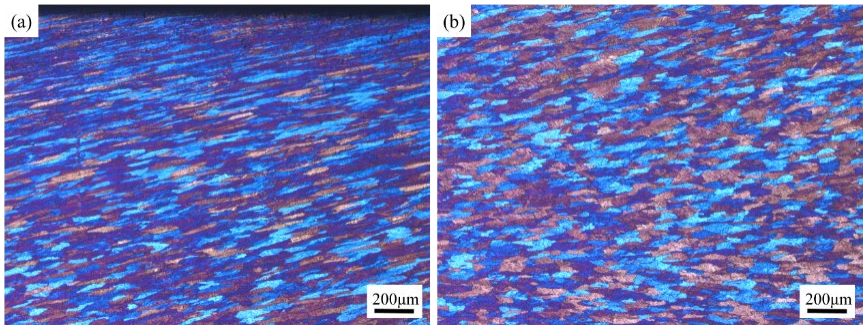

Figure 2 Grain structure of 6.0 mm cast-rolling billet: (a) edge; (b) Core

The secondary phase structure of the 6.0 mm cast-rolled blank is shown in Figure 3. Figure 4(a, c) displays the secondary phases at the edge of the cast-rolled sheet, revealing a fine strip-like distribution with partial fragmentation into continuous granular secondary phases. The elongation direction of these strips aligns with the elongated grain orientation, as observed in the grain structure images.

Figure 1-3(b, d) illustrates the secondary phase distribution in the core region of the 6.0 mm cast-rolled sheet, which exhibits a continuous dendritic network morphology distinct from the edge. Table 1 provides the elemental analysis of secondary phases in the edge and core regions, confirming their composition as primarily Al and Fe, with trace amounts of Si detected, consistent with Al-Fe binary eutectic phases.

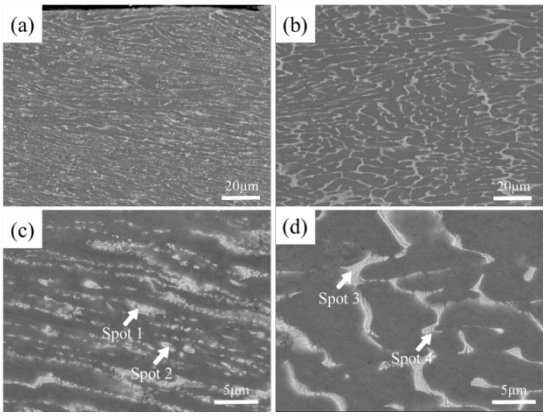

Figure 3 SEM image of 6.0mm cast-rolling blank: (a) edge; (b) Core

Table 1 The EDS analysis results of the second phase particles

	Al(wt.%)	Fe(wt.%)	Si(wt.%)
Spot 1	94.51	5.20	0.29
Spot 2	92.88	6.84	0.28
Spot 3	91.89	7.85	0.26
Spot 4	91.37	8.33	0.30

3.2 Microstructural Analysis of 4.2 mm Pre-Deformed Sheet Before and After Homogenization Annealing

The 6.0 mm cast-rolled blank was first pre-deformed by 30% to obtain a 4.2 mm pre-deformed sheet, followed by homogenization annealing at different temperatures. The RD-ND plane was anodized and observed under 50× optical magnification. Figure 4 shows the grain distribution of the 4.2 mm sheet before and after homogenization annealing. In Figure 4(a) (H18, unannealed sample), grains are elongated along the rolling direction (increased grain size along RD and decreased along ND). Figures 4(b-d) display the anodized images of the pre-deformed sheet after homogenization annealing at 500°C, 540°C, and 580°C for 3 h, respectively. For the 500°C annealed sample (Figure 4b), grain size increased significantly, with edge grains along RD being larger than those in the core. After 540°C annealing (Figure 4c), coarse recrystallized grains emerged in certain regions due to microstructural inhomogeneity. For the 580°C annealed sample (Figure 4d), grains were uniformly distributed with minimal edge-core

ISSN 2616-5880 Vol. 6, Issue 2: 17-24, DOI: 10.25236/AJMC.2025.060202

differences, accompanied by smaller recrystallized grains. Figure 5 summarizes the grain size statistics, showing that homogenization annealing increased grain size overall, but no significant variation occurred with rising annealing temperatures.

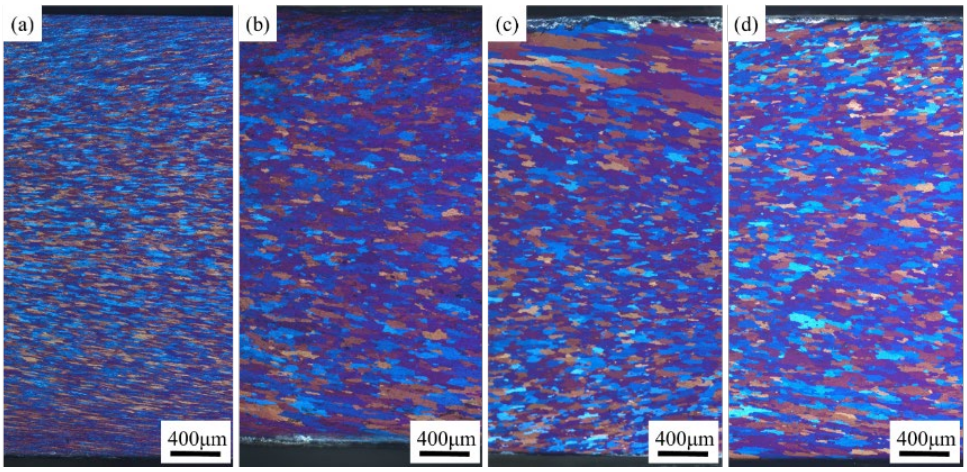

Figure 4 Grain structure of 4.2mm cold-rolled sheet: (a)H18; (b)500 ℃ /3h; (c) 540℃/3h and (d) 580℃/3h homogenizing annealing

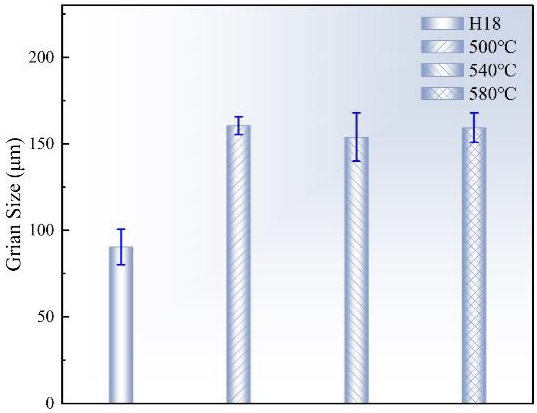

Figure 5 Grain size of 4.2mm sheet with different homogenization annealing

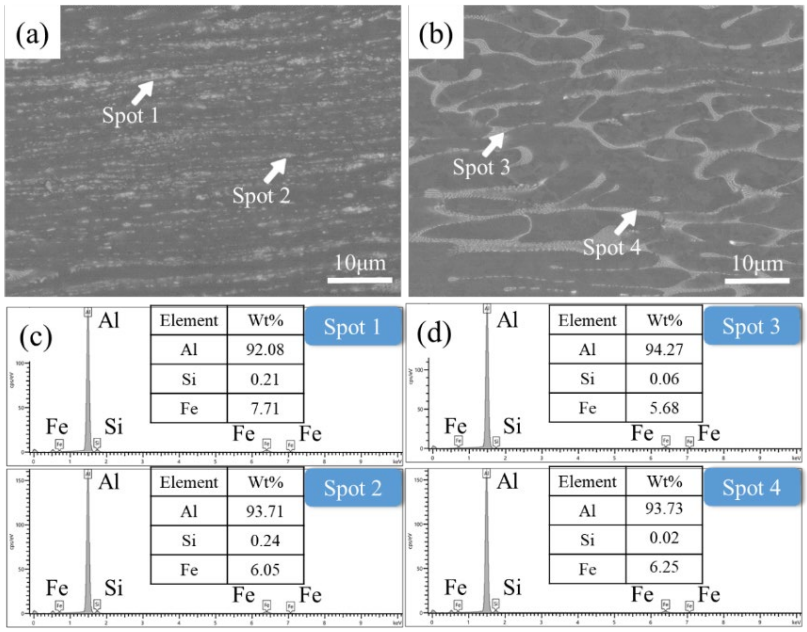

Figure 6 SEM(a) side of 4.2mm pre-deformed cold-rolled sheet; (b) core, and EDS(c) side; (d) Core

ISSN 2616-5880 Vol. 6, Issue 2: 17-24, DOI: 10.25236/AJMC.2025.060202

Figure 6 shows the BSE and EDS analysis of the 4.2 mm thick 8021 cold-rolled sheet before homogenization annealing. (a) displays the secondary phase distribution in the edge region of the cold-rolled sheet. After 30% cold rolling, the edge secondary phases retain a strip-like distribution, with further reduced interstrip spacing along the thickness direction. (b) illustrates the secondary phase distribution in the core region of the cold-rolled sheet. The morphology of the core secondary phases remains unchanged after cold rolling, exhibiting a network-like structure distinct from the edge region.(c, d) present the EDS analysis of the edge and core secondary phases. Both strip-like (edge) and network-like (core) secondary phases consist of Al, Fe, and Si. Trace amounts of Si are detected in the edge strip-like phases, while Si content in the core network-like phases is nearly zero. This confirms that the secondary phases in both edge and core regions are Al-Fe binary phases.

Figure 7 presents the BSE images of the sheet under different homogenization annealing temperatures, and Table 2 summarizes the EDS results of the secondary phases. After annealing at 500℃, the strip-like secondary phases in the surface region nearly disappear, with dissolution of the original Al-Fe metastable phases. Based on phase contrast and morphology, apart from the re-dissolution of dendritic primary secondary phases, granular dispersed phases begin to precipitate. In the core region, some primary phases remain in the network structure, and the area fraction of secondary phase particles in eutectic regions significantly decreases. Similar to the edge region, blocky and granular dispersed phases also appear in the core.

Figures 7(b, c) show the secondary phase distribution after 540℃ annealing. The strip-like secondary phases in the surface region completely vanish. Combined with EDS results, the short rod-shaped phase labeled as point 6 exhibits an Fe/Si ratio exceeding 1.5, identifying it as β-AlFeSi phase based on morphology. Small portions of the network-like secondary phases persist in the core region.

After annealing at 580℃, the secondary phase distribution differs markedly from that of the 540℃ annealed sheet. Notably, the precipitation of secondary phases increases, with more granular phases and numerous fine needle-like secondary phases observed. The core and edge regions show no distinct differences in secondary phase distribution, indicating improved uniformity.

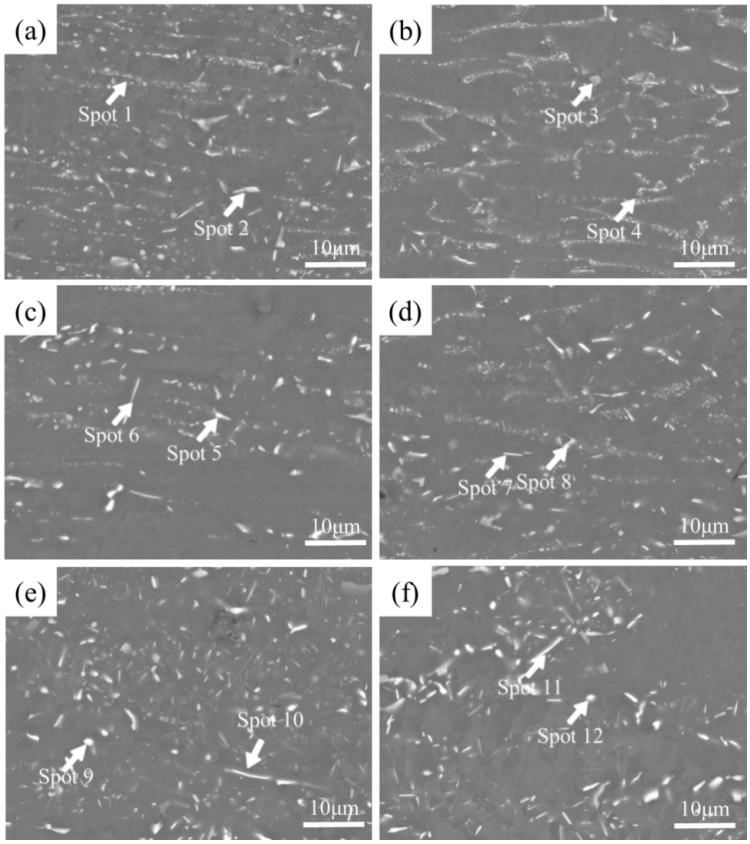

Figure 7 SEM images of the (a, c and e) sides and (b, d and f) cores of 4.2mm plates under different annealing treatments, (a, b) 500℃/3h, (c, d) 540℃/3h and (e, f) 580℃/3h

ISSN 2616-5880 Vol. 6, Issue 2: 17-24, DOI: 10.25236/AJMC.2025.060202

Table 2 The EDS analysis results of the second phase particles are shown in Figure 7

	Al(wt.%)	Fe(wt.%)	Si(wt.%)
Spot 1	90.00	10.00	0
Spot 2	89.45	10.47	0.07
Spot 3	94.44	5.47	0.04
Spot 4	89.80	9.99	0.21
Spot 5	88.80	10.22	0.99
Spot 6	97.30	1.69	1.01
Spot 7	90.07	9.90	0.03
Spot 8	85.20	14.74	0.07
Spot 9	78.36	21.53	0.11
Spot 10	87.08	12.84	0.08
Spot 11	87.38	12.54	0.08
Spot 12	86.14	13.78	0.08

The phase transformation mechanism of secondary phases in aluminum alloys follows a dissolution-precipitation process, where the composition and distribution of secondary phases are governed by atomic diffusion. Under identical concentration gradients, the rate of diffusion is determined by the diffusion coefficient DD. The expression for DD is given by Equation (1).

$$D = D_0 \exp\left(-Q/RT\right) \tag{1}$$

In the formula, D_0 is the diffusion constant; Q is the diffusion activation energy; R is the gas constant; T is the thermodynamic temperature. There are many factors that affect the diffusion coefficient, such as the type of solid solution, crystal structure and temperature, etc. However, among these factors, temperature has the greatest impact on diffusion in the same material. Therefore, the higher the temperature, the more complete the atomic diffusion. As a result, with the increase of annealing temperature, more and more second phases dissolve and the diffusion distance becomes longer. In aluminum alloys, the atomic radius of Fe is larger than that of Si, so the diffusion activation energy required for Fe diffusion is greater than that of Si. Generally, in aluminum alloys, the diffusion distance of Si can be very long, while the diffusion distance of Fe is often around the original second phase.

When annealed at 500°C, Al_6Fe begins to dissolve, and the second phase between the eutectic and dendrites further disappears. At the same time, a large amount of Fe atoms are dissolved in the aluminum matrix around the dendrite boundaries. During cooling, fine Al3Fe will precipitate. When annealed at 540°C, a large amount of binary metastable phases dissolve, so the eutectic phase basically disappears. Due to the further dissolution of Fe, Fe atoms will aggregate around the previously large and insoluble needle-like and plate-like Al_3Fe, causing it to grow and coarsen. At the same time, some Fe atoms will precipitate extremely fine needle-like Al_3Fe. The dissolution of the ternary phase β_p will reduce the size of the blocky second phase.

When annealed at 560°C, only a small amount of Al_6Fe remains in the binary metastable phase. At this time, Al_3Fe partially grows, and the further dissolution of the metastable phase provides more Fe atoms. The solubility of Fe atoms in the Al matrix is limited, and the excess Fe atoms will precipitate new Al_3Fe. The diffusion distance of Fe atoms in the Al matrix is limited, and it increases with the increase of temperature [7]. The newly precipitated Al3Fe phase is more dispersed. The transformation of β_p to β_b depends on the diffusion of Si atoms in the solid solution [8], and the diffusion distance of Si is relatively long.

Therefore, small-sized granular and short rod-shaped second phases appear in the originally second-phase-free intragranular regions, which are the newly precipitated β_b phases. By this point, the distribution of the second phase is roughly uniform after annealing at 560°C, and the second phase originally forming a network around the dendrites is completely eliminated. The higher the temperature, the more complete the atomic diffusion, and the more uniform the distribution of the second phase. However, the annealing temperature should not exceed 560°C. If the temperature continues to rise, needle-like Al_3Fe will continue to precipitate and the original Al3Fe will continue to grow and coarsen. This will cause stress concentration during subsequent rolling and reduce the formability of the slab, affecting the subsequent rolling process.

3.3 Grain size and performance analysis of cold-rolled 1.0mm thin plates

The pre-deformed plates from 6.0mm billets were not annealed and were uniformly annealed at

ISSN 2616-5880 Vol. 6, Issue 2: 17-24, DOI: 10.25236/AJMC.2025.060202

500°C, 540°C, and 580°C. The total deformation amount of the cold-rolled 1.0mm plates without annealing reached 83.3%. The grain size data of the 1.0mm thickness samples after uniform annealing of the pre-deformed plates are shown in Figure 8. The higher the uniform annealing temperature of the pre-deformed plates, the smaller the grain size of the 1.0mm thickness samples. The mechanical properties are shown in Table 3.

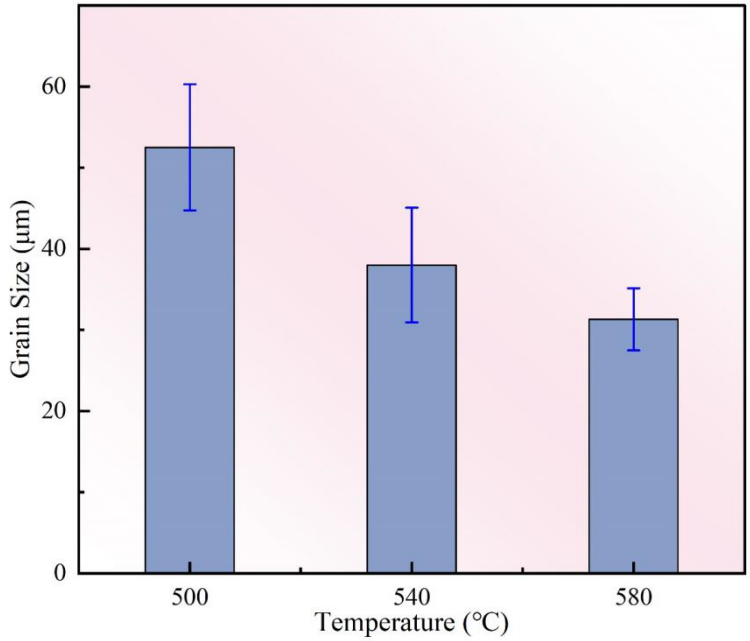

Figure 8 Grain size statistics of annealed sheet rolled at 6.0 mm (temperature is the homogenization temperature of predeformed sheet)

Table 3 1.0 mm final sheet mechanical properties

	H18	500°C	540°C	580°C
Tensile strength(MPa)	178.2	113.8	118.4	125.4
Yield strength(MPa)	160.49	59.81	60.92	62.34
Rate of elongation(%)	9.24	18.41	20.62	22.32

It can be seen that the tensile strength of the H18 state sample reached 178.2 MPa, and the elongation was 9.24%. Its tensile strength and yield strength were much higher than those of other thin plates, but the elongation was the lowest. This is because the grain structure of the final thin plate in the H18 state was still in a deformed state, with only the core area partially recrystallized. At this time, the thin plate had a high degree of work hardening, resulting in high strength and low elongation. After uniform annealing, the tensile strength of the sheet was between 110 MPa and 130 MPa, and the elongation was between 18% and 23%. As the annealing temperature increased, the strength and elongation of the final thin plate also increased.

4. Results and discussion

(1) The microstructure of the 6.0mm cast-rolled plate is not uniform in the thickness direction, the surface layer shows elongated rolled grains and strip second phase, the grain elongation in the core region is much less than the surface layer, and the second phase is a network structure. After annealing, recrystallization occurs, and the difference of grain and second phase morphology between surface and core regions decreases.

(2) With the increase of homogenization temperature, the grain size of the final 1mm sheet gradually decreases, mainly due to the differences in grain size after pre-annealing of the cast-rolled sheet, and these differences continue to the final sheet in the subsequent deformation;

(3) The final sheet rolled by annealed predeformed sheet has the highest strength and the lowest elongation, and the tensile strength of annealed predeformed sheet rolled by annealed predeformed sheet is 110 MPa~130 MPa, and the elongation is 18%~23%. With the increase of annealing temperature, the

ISSN 2616-5880 Vol. 6, Issue 2: 17-24, DOI: 10.25236/AJMC.2025.060202

grain size of the material is refined, and the fine grain strengthening effect makes the strength and elongation increase.

References

[1] Chen Z W, Li S S, Zhao J. Homogenization of twin-roll cast A8006 alloy[J]. 2012,22:1280-1285.
[2] Engler O, Laptyeva G, Wang N. Impact of homogenization on microchemistry and recrystallization of the Al-Fe-Mn alloy AA 8006[J]. 2013,79:60-75.
[3] Chayong S, Atkinson H V, Kapranos P. Multistep induction heating regimes for thixoforming 7075 aluminium alloy[J]. Metal Science Journal, 2004,20:490-496.
[4] Ivanisenko Y V, Korznikov A V, Safarov I M, et al. Formation of submicrocrystalline structure in iron and its alloys after severe plastic deformation[J]. Nanostructured Materials, 1995,6:433-436.
[5] Korznikov A V, Ivanisenko Y V, Laptionok D V, et al. Influence of severe plastic deformation on structure and phase composition of carbon steel[J]. Nanostructured Materials, 1994,4:159-167.
[6] Birol Y. Recrystallization of twin-roll cast Al–Fe–Si foil stock processed without homogenization[J]. 2009,488:112-116.
[7] Kumar R, Gupta A, Dandekar T R, et al. Evolution of microstructure and texture during homogenization in a strip cast AA8011 aluminum alloy[J]. 2021,130.
[8] Králik R, Křivská B, Bajtošová L, et al. The influence of Zener drag on recrystallization behaviour of twin-roll cast AA8079 alloy after homogenization[J]. 2021,1178:12034-12039.